Determination of the minimum value of the safety factor from geodesic Alfvén eigenmodes in Joint European Torus

A. G. Elfimov,[1,a)] R. M. O. Galvão,[1,2] S. E. Sharapov,[3] and JET-EFDA Contributors[b)]
JET-EFDA, Culham Science Centre, Abingdon OX14 3DB, United Kingdom
[1]*Institute of Physics, University of São Paulo, 05508-090 São Paulo, Brazil*
[2]*Centro Brasileiro de Pesquisas em Física, Rua Xavier Sigaud 150, BR-22290180 Rio de Janeiro, Brazil*
[3]*Euratom/CCFE Fusion Association, Culham Science Centre, Abingdon OX14 3DB, United Kingdom*

(Received 22 June 2010; accepted 7 September 2010; published online 9 November 2010)

An analysis of the experimental conditions under which low-frequency (70–150 kHz) Alfvén eigenmodes (AE) are excited during the monster sawtooth in Joint European Torus [F. Romanelli *et al.*, Proceedings of the 22nd IAEA Fusion Energy Conference, Geneva, Switzerland, 2008] is presented for the specific case of a discharge with ion cyclotron heating (5 MW). Using a simplified AE model for modes excited at the Alfvén wave continuum maximum with geodesic corrections taken into account, the temporal evolution of the value of the safety factor q_0 at the magnetic axis is determined. We describe a new scheme to determine the time variation of q_0 that works under conditions in which other standard diagnostics, such as the motional Stark effect do not give reliable results such as during a monster sawtooth. [doi:10.1063/1.3494212]

A number of low frequency Alfvén waves (AW),[1] such as the toroidicity induced Alfvén eigenmode (TAE),[2] Alfvén cascade (AC),[3] tornado,[4] sierpes modes,[5] etc., have been observed during ion cyclotron heating (ICRH) and/or neutral beam injection in different tokamaks. These modes have attracted wide interest[1,3–6] because of the enhanced transport of energetic ions induced by them and their possible usage as a diagnostic tool, especially, to determine the profile of the safety factor q in the plasma core in discharges with sawteeth. One specific mode appears in the low frequency band (70–100 kHz) during high power (~5 MW) ICRH discharges with high electron temperatures (~8 keV) and peaked radial profile in the Joint European Torus[7] (JET). The mode manifests as an AC with the dispersion relation modified by geodesic corrections, and toroidal mode number $N=1$. The theory of AC was well developed for reversed shear plasmas[8] taking into account the geodesic effect[9] and pressure corrections.[10] However, no experimental indications of reversed shear profiles, which are a condition for AC, have been found in this discharge. We therefore revisit the theory to describe the observed mode. Typically, Alfvén eigenmodes (AE) may appear at the minimum or maximum of the Alfvén wave continuum (AWC). The geodesic corrections modify AWC[9–13] to the form

$$\omega_{\mathrm{GA}} = \frac{\omega_i^*}{2} + \sqrt{(c_A k_N)^2 + \omega_{\mathrm{geo}}^2}, \tag{1}$$

where

$$\omega_{\mathrm{geo}}^2 \approx \left[\frac{7}{2} + 2\frac{T_e}{T_i} + \left(\frac{23}{8} + 2\frac{T_e}{T_i} + \frac{T_e^2}{2T_i^2}\right)\frac{\mathrm{v}_{\mathrm{Ti}}^2}{q^2 R_0^2 \omega_{\mathrm{geo}}^2}\right]\frac{\mathrm{v}_{\mathrm{Ti}}^2}{R_0^2},$$

$c_A = B/\sqrt{4\pi n_i m_i}$ is the Alfvén speed, $k_N = B_\zeta / BR_0(N + M/q)$, $v_{Te,i} = \sqrt{T_{e,i}/m_{e,i}}$ is the electron or ion thermal speed, M and N are poloidal and toroidal mode numbers, respectively, $\mathbf{B}$ is the magnetic field, R_0 is the major radius, q is the safety factor, and ω_{geo} is the geodesic frequency. The AE propagation at the AWC extremum depends strongly on the relation between gradients of plasma pressure and the magnetic shear.[14] When the plasma pressure gradients are strong, the AE may propagate at the maximum of the AWC; however, if the pressure gradients are weak, the modes may appear at AWC minimum. Here, we note that eigenmodes at extremum points of the lower branches of the geodesic AWC $\omega \ll \omega_{\mathrm{geo}}$ were studied in Ref. 15.

In this work, we analyze the experimental conditions for AE excitation in the 70–150 kHz frequency band that appear during a monster sawtooth in JET discharge 66209 and demonstrate the occurrence of a robust on-axis AC eigenmode above the Alfvén continuum in tokamak discharges with the minimum value of q on the magnetic axis. The characteristics of this discharge are similar to those of 66203 discussed in Ref. 6. Taking into account the geodesic corrections due to poloidal mode coupling in tokamaks, the quasicylindrical model[13,14] is used to clarify the existence of the AE at the AWC maximum.

The parameters of the discharge nos. 66203 and 66209 were magnetic field 2.7 T, plasma current 2 and 1.8 MA, central electron temperature 7 and 8 keV, density 3.4 and 3.2×10^{19} m^3, and ICRH power of 4.5 and 5.3 MW, respectively. Figure 1 shows the time evolution of the electron temperature, and line-average electron density at the beginning of ICRH $t=10$ s in JET discharge no. 66209. The corresponding waveforms for the 66203 shot are presented in

a)Electronic mail: elfimov@if.usp.br.
b)See the Appendix of F. Romanelli *et al.*, Proceedings of the 22nd IAEA Fusion Energy Conference 2008, Geneva, Switzerland.

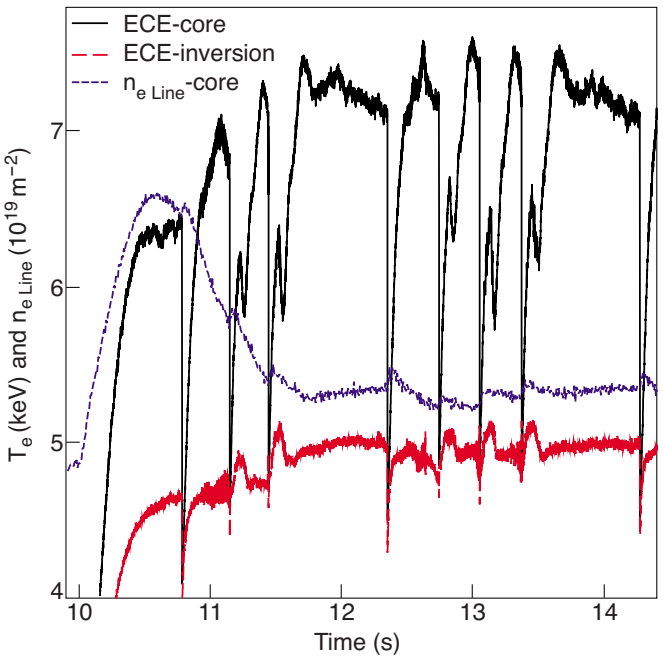

FIG. 1. (Color online) Time trace of electron temperature measured by ECE at the plasma core (upper line), and at the inversion radius (≈0.31 m) marked by a gray color at the beginning of the ICRH pulse. The intermediate traced black line reproduces data of the core line interferometer.

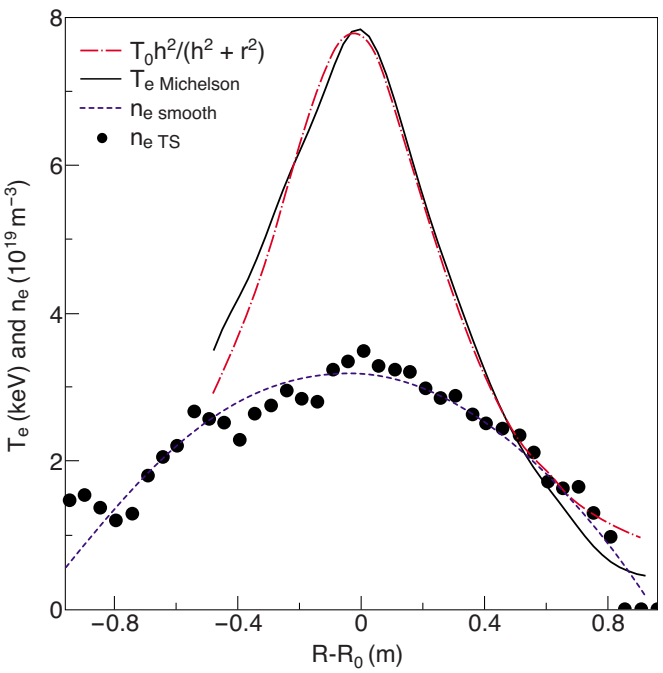

FIG. 2. (Color online) Plot of electron temperature (solid) and their analytic model (chain line) at $t=13.65$ s. Black circles and dotted line, respectively, mark the electron density from Thomson scattering and its smoothed profile (parabolic).

Ref. 6. For the next analysis, we chose the monster sawtooth shown in Fig. 1 at $t=13.5-14$ s, because of the rather small density variation during this time interval. The peaked electron temperature radial profile fitted with the expression $T_0h^2/(r^2+h^2)$, where r is the minor radius (half-width ≈33 cm), and the parabolic density profile at $t=13.65$ s are shown in Fig. 2. A mild temporal decrease of the temperature maximum, $\delta T/T_0=4,5\%$, is observed due to the fast ion loss driven by the tornado modes[6] before the sawtooth crash. We note that the ion temperature was not measured in this discharge; however, its value is expected to be of the order of 4.3 keV, as measured in the similar 66203 discharge and indirectly confirmed in calculations of the geodesic frequency ω_{geo} for no. 66209.

The spectrograms of the magnetic probe and of the O-mode reflectometry signals are shown in Figs. 3(a) and 3(b) in the time widow 13.35–14.3 s. The $N=1$ AE is clearly visible in the magnetic signals during the monster sawtooth but the AC is only registered by reflectometry. This 50.47 GHz reflectometry channel has a density cut of $\approx 3.16\times 10^{19}$ m^{-3} and the central plasma density is very close to the cutoff value, what helps to localize the mode at the plasma core. Similar AE behavior[16] was recently observed in ASDEX experiments. The $N=1$ mode is also visible in spectrograms of two central soft x-ray channels at the magnetic axis but it is absent in other channels. These data together with reflectometry indicate that the mode position is very close to the magnetic axis. In the corresponding spectrogram of 66203 shot, the $N=1$ mode appears in the magnetic probe spectrogram but it is not reproduced in the O-mode reflectometry channel, due to the higher central density. However tornado modes[6] are observed because of their positions, which are closer to $q=1$ magnetic surface, confirming the idea of core position of the $N=1$ mode. We note that all parameters discussed here $T_{ie}(t)$, frequency $f(t)$, $q_0(t)$, and deviation $\delta q(t)$ depend on time during a sawtooth but this functional dependence is omitted.

Comparing Fig. 1 with Fig. 3(b), we can observe that the spontaneous AC chirping in the time interval $t=13.5-13.7$ s is correlated with the increase in the electron temperature, which is driven by the fast ions, and is accom-

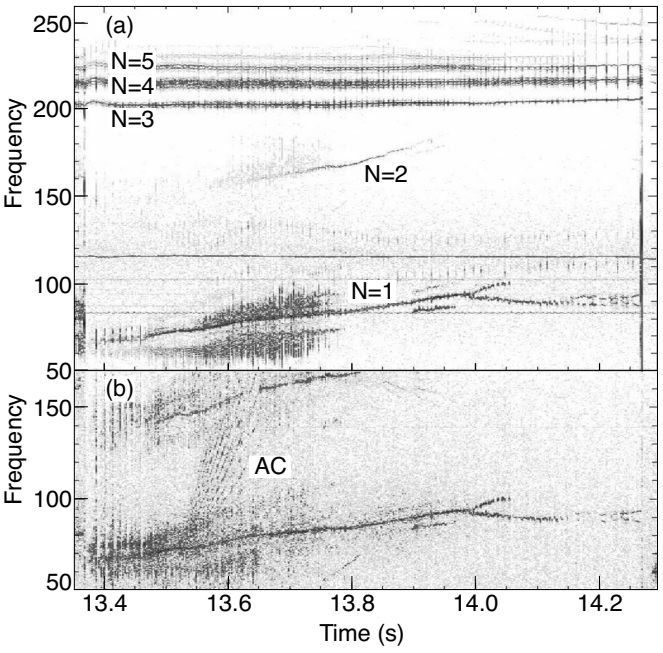

FIG. 3. Spectrogram of magnetic probe signal (a) and 50.5 GHz channel of O-mode reflectometry (b).

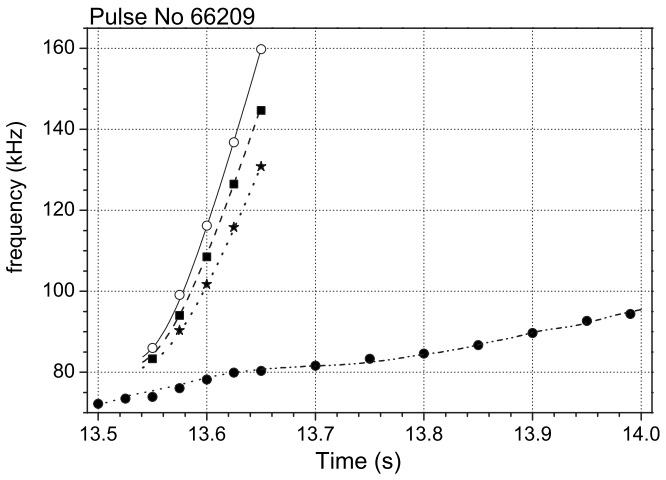

FIG. 4. Plot of $N=1,6,7,8$ AC spectra calculated from Eq. (1) shown, respectively, by dash-dot-dotted, dotted, dashed, and solid lines in comparison with the AC spectra tracked from Fig. 3(b) shown by black points, stars, black squares, and open circles, respectively.

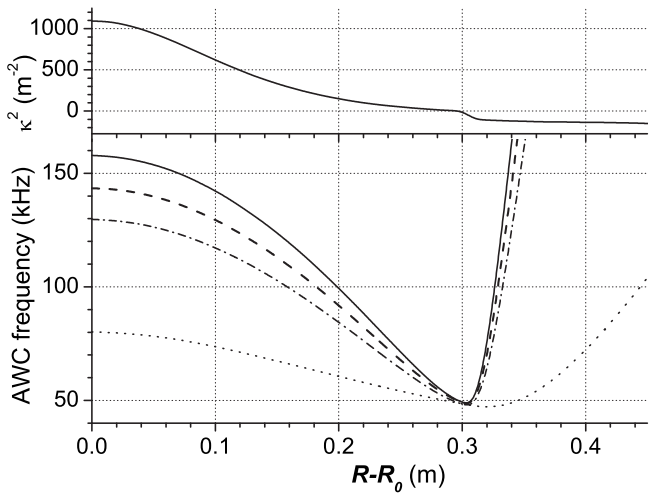

FIG. 5. Plot of the geodesic AWC for $N=1,6,7,8$ (dotted, dash-dotted, dashed, and solid lines, respectively), and κ^2 profile (upper part) for $N=1$ at $t=13.65$ s.

panied by the slow increase of $N=1$ AE frequency of $\delta f/f=9\%$, which may be also attributed to the electron temperature. Using the above results, we may attempt to calculate the q_0-evolution by measuring the evolution of the $T_{i,e}$-values and tracking the AC mode frequencies from Fig. 3 during the respective time interval. However, we show below that this method has accuracy limitations immediately after the sawtooth crash, what can be partially overcome by analyzing the AC modes at $t=13.55-13.65$ s.

First, we propose that the $N=1$ mode has the same origin as the AC, which have high toroidal mode numbers. Employing the idea of AC excitation at the maximum of AWC, and representing $k_N=N\delta q/R_0q_0$, where $\delta q=1-q_0$ and $M=-N$, we subtract drift term in Eq. (1) and represent the frequency difference between the AC modes for the N and N_1 toroidal numbers as $\omega_{N1}/N_1-\omega_N/N\approx\sqrt{(\omega_{\text{geo}}/N_1)^2+(c_A\delta q/R_0q_0)^2}-\sqrt{(\omega_{\text{geo}}/N)^2+(c_A\delta q/R_0q_0)^2}$. Second, the $N=1$, 6–8 AC spectra in Fig. 3 are tracked and the corresponding values are represented by the points in Fig. 4 in the time interval $t=13.55-13.65$ s. Then, q_0 and ω_{geo} are calculated for the respective time moments using frequency combinations between the observed AC modes in the above equation. As a result of the calculations, the q_0-time variation is represented by the expression $q_0(t)=0.995-0.35\cdot(t-13.55)$ with ±0.002 deviation. Then, the $N=1$, 6–8 AC spectra are recalculated using the T_{e0} time dependence shown in Fig. 1 together with the obtained $q_0(t)$-equation, and assuming $T_{i0}/T_{e0}=$const in accordance with the similar discharge no. 66203 where T_{i0} was measured. The respective results are plotted as the dash-dotted, dotted, dashed, and solid lines in Fig. 4. We observe that there is quite good agreement with the respective trucked data, confirming the $T_{i0}/T_{e0}=$const model taken from the discharge no. 66203. For $t=13.65$, we found $\delta q\approx0.04\pm0.002$, the respective $M=1$ drift frequency $f_1^*\approx1.5\pm0.5$ kHz, $f_{\text{geo}}\approx78.1\pm0.8$ kHz from where the ion temperature at 4.8 keV is calculated. In this case, the Doppler shift frequency due to rotation is estimated less then 0.3 kHz.

After that moment, the AC modes disappear, the electron temperature begins to slightly decrease but the $N=1$ mode frequency increases further, arriving at $\delta f/f=18\%$ at $t=14$ s, which indicates strong decrease of q_0. The procedure developed above for the δq calculation gives us an opportunity to apply it for the time interval $t=13.65-14$ s when we only have the T_{e0}-evolution and the $N=1$ spectrum. Using $T_{i0}/T_{e0}=$const with the deviation error of 3% taken from the discharge no. 66203, and $f_{\text{geo}}\approx78.1$ as a reference point at $t=13.65$, we calculate the f_{geo} values at instant of time related to the tracked $N=1$ spectrum shown in Fig. 4 obtaining $f_{\text{geo}}\approx76.6$ kHz at $t=14$ s. Next, we calculate the drift frequency using the ion temperature profile $T_{i0}(1-2\cdot r^2/a^2)$ with the deviation of 4% in the plasma core, as it was found in the discharge no. 66203. Finally, substituting these data into Eq. (1), the q_0-time evolution is calculated for the tracked points, which result is fitted by the expression $q_0(t)=0.96-0.284\cdot(t-13.65)$ with the ±0.003 deviation for the interval $t=13.65-14$ s giving $q_0=0.86$ at $t=14$ s. Then, the mode splits into two branches, possibly due to a precursor rotation, and the high branch disappears, making it difficult the prediction of the q variation.

The best accuracy of the δq-estimation is about 5% at $t=13.65$ s and it is mainly limited by the accuracy of central density measured by Thomson scattering; however, the accuracy worsens to 12%–14% at $t=14$ s due to the imprecision in the ion temperature, which can only be estimated from the data of the discharge no. 66203. The prediction of the q_0-value immediately after the sawtooth crash has a problem due to very small difference between the $f_{N=1}$ and f_{geo} frequencies, which produces a large relative error due to imprecision on the values of the density and of the ratio T_e/T_i.

In Fig. 5, to visualize the AE frequencies at the maxima of the geodesic AWC in Eq. (1), we plot the continua for $N=1,6,7,8$ at the moment $t=13.65$ s, where the electron temperature and density profiles shown in Fig. 2 are used. The respective maxima of the frequency appear very near to the eigenmode frequencies shown in Fig. 3. Here, it is pro-

posed that q-profile does not change between inversion radius r_{in} and plasma border $r=a$, $q(r)=1-(q_a-1)(r^2/r_{in}^2-1)$ that is in accordance with practically constant TAE's frequencies for $N=3-6$ shown in Fig. 3. After the sawtooth crash at $t=13.4$ s, the q-profile variation is assumed as $q(t)=1-\delta q(t)(1-(r/r_{in})^2$ from the magnetic axis to the inversion radius for the period 13.5–14.2 s.

To confirm the existence of AE at maximum of the AWC, we use the kinetic model for plasmas[13] with hot electrons and cold ions, $v_{Te} \gg \omega R_0 \gg v_{Ti}$, in the quasicylindrical tokamak geometry $r \ll R_0$, which is satisfactory to describe the AC in the plasma core of JET. The approach[13,14] helps us to reduce the Maxwell equations to the Hain–Lust form

$$\frac{1}{r}\frac{d}{dr}\left(rD\frac{dF}{dr}\right)+\left[Q-\frac{M^2D}{r^2}\right]F=0, \tag{2}$$

where

$$D=(\omega^2-\omega_{geo}^2)/c_A^2-k_M^2=0,$$

$$Q=\frac{M}{r}\frac{d}{dr}[2k_M/R_0q+(\omega_i^*-\omega_e^*)\omega_{ci}/c_A^2],\quad F=rE_b,$$

$\omega_\alpha^*=(k_b/\omega_{c\alpha}n_\alpha)(\partial/\partial r)(v_{T\alpha}^2 n_\alpha)$ is the drift frequency, $k_b \approx M/r$, and the equation $D=0$ describes the geodesic Alfvén wave continuum presented in Eq. (1). Equation (2) looks like the Bessel equation and its formal solution may be presented in the eikonal form $F=F_0J_m(\int_0^r \kappa dr)$ where $\kappa=\sqrt{Q/D}$ should be large $(\kappa^2 r_f^2 \gg 1)$. For the density and temperature profiles shown in Fig. 2, the Q-function is positive and it has a maximum at $r=0$ where the D-function is positive for the frequency above the continuum. Here, we note that Q-function is positive due to the second "drift" term in the plasma core that is much large than the fist term related to the shear due to the sharp electron temperature profile in this discharge. To have an eigenmode solution, the D-function should be positive independent of the shear profile, which may be positive or negative in the plasma core. The Q-function decreases with radius and it may change sign giving a reflection point for AE at $r=r_f$ defined by the next implicit equation

$$Q \approx 4M^2\left(\frac{\beta_0 h^2}{(h^2+r_f^2)^3}-\frac{1}{r_f q^3 R_0^2}\left.\frac{dq}{dr}\right|_{r=rf}\right)=0, \tag{3}$$

where $\beta_0=8\pi n_0(T_{i0}+T_{e0})/B_0^2$. It should be noted that the reflection point coincides with the radius of $q=1$ magnetic surface due to bending of q-profile just after the sawtooth crash but it may stay closer to magnetic axis in the case of an incomplete sawtooth crash[17] when the $q<1$ small region is preserved at the plasma core. Later, the reflection point moves out from this surface due to smoothing of q-profile, when the approximation $q=q_0+(q_a-q_0)r^2/a^2$ can be used. Matching the solution of Eq. (2) with Airy solution at the reflection point, we get the quantization rule for the AE eigenvalues, $\int_0^{rf}\kappa dr=(|M|/2+s)\pi$, where $s=1,2,3\ldots$. This equation is valid for AC as well as for the $N=1$ AE mode. We understand that the WKB presentation gives only a qualitative result for the case of the eigenvalue. Moreover, finite integration of this expression is not possible and a direct numerical solution of Eq. (2) is employed to find the respective eigenvalues. Assuming the position of the reflection point at the $q=1$ rational surface $r_f=0.3$ m and solving Eq. (2) for $h=0.33$ m in Fig. 2, and the respective $N=1$ AWC profile shown in Fig. 5 at $t=13.65$ s, we find that the $N=1$ AE frequency is $\omega=\omega_{GA}+\Delta\omega$ where $\Delta\omega/\omega=0.013$. For this frequency, the respective κ^2 profile is shown in the upper plot of Fig. 5. The discrepancy between the WKB approximation and the numerical result is found $\approx 30\%$. Numerical calculations demonstrate that 20% variation of the reflection point position produces not more then 30% variation of $\Delta\omega$, a value that is satisfactory enough for our method of the eigenfrequency identification as the frequency of the AWC maximum. The behavior of the eigenfunction is very similar to the above asymptotic solution. It has maximum at $r_m=0.75h\sqrt{\Delta\omega/\omega}$, then, it begins to drop exponentially for $r>3r_m$.

Finally, we conclude that the spectral analysis of the low $N=1$ Alfvén eigenmodes, as well as high N-chirping AC eigenmodes observed during ICRH in JET discharges with the monotonic q-profiles, may help determination of the q_0-value at the magnetic axis taking into account the geodesic frequency. This method allows accompanying the q_0-variation during sawtooth discharges, what is very difficult to do employing standard diagnostics such as motion Stark effect.

This work, supported by the European Communities under the contract of Association between EURATOM and Brazil, was carried out within the framework of the European Fusion Development Agreement. First two authors are thankful to CNPq (National Council of Brazil for Science and Technology Development) for financial support.

[1] K. L. Wong, Plasma Phys. Controlled Fusion **41**, R1 (1999).
[2] H. H. Duong, W. W. Heidbrink, E. J. Strait *et al.*, Nucl. Fusion **33**, 749 (1993).
[3] S. E. Sharapov, D. Testa, B. Alper *et al.*, Phys. Lett. A **289**, 127 (2001).
[4] M. Saigusa, H. Kimura, Y. Kusama *et al.*, Plasma Phys. Controlled Fusion **40**, 1647 (1998).
[5] M. García-Muñoz, H.-U. Fahrbach, S. Günter *et al.*, Phys. Rev. Lett. **100**, 055005 (2008).
[6] P. Sandquist, S. E. Sharapov, M. Lisak, and T. Johnson, Phys. Plasmas **14**, 122506 (2007).
[7] S. E. Sharapov, B. Alper, Yu. F. Baranov *et al.*, *Proceedings of the 21st International Conference on Fusion Energy* 2006, Chengdu (IAEA, Vienna, 2006), p. EX/P6-19.
[8] H. L. Berk, D. N. Borba, B. N. Breizman, S. D. Pinches, and S. E. Sharapov, Phys. Rev. Lett. **87**, 185002 (2001).
[9] B. N. Breizman, M. S. Pekker, S. E. Sharapov, and JET EFDA Contributors, Phys. Plasmas **12**, 112506 (2005).
[10] G. Y. Fu and H. L. Berk, Phys. Plasmas **13**, 052502 (2006).
[11] H. Sugama and T.-H. Watanabe, Phys. Plasmas **13**, 012501 (2006).
[12] F. Zonca and L. Chen, EPL **83**, 35001 (2008).
[13] A. G. Elfimov, Phys. Plasmas **17**, 022102 (2010).
[14] A. G. Elfimov, C. J. A. Pires, and R. M. O. Galvão, Phys. Plasmas **14**, 104506 (2007).
[15] N. N. Gorelenkov, H. L. Berk, N. A. Crocker *et al.*, Plasma Phys. Controlled Fusion **49**, B371 (2007).
[16] P. Lauber, M. Brüdgam, D. Curran *et al.*, Plasma Phys. Controlled Fusion **51**, 124009 (2009).
[17] F. Porcelli, D. Boucher, and M. N. Rosenbluth, Plasma Phys. Controlled Fusion **38**, 2163 (1996).